NASA TECHNICAL MEMORANDUM

37

REPORT NO. 53913

STATISTICAL THEORY OF INELASTIC NEUTRON ENERGY SPECTRA

By B. J. Henderson and C. E. Wuller, Jr.
Space Sciences Laboratory

September 16, 1969

NASA

George C. Marshall Space Flight Center
Marshall Space Flight Center, Alabama

IN-SSL-N-68-14

Changed to TM X-53913, September 16, 1969

STATISTICAL THEORY OF INELASTIC NEUTRON ENERGY SPECTRA

By

B. J. Henderson and C. E. Wuller, Jr.

George C. Marshall Space Flight Center

ABSTRACT

A statistical theory of inelastic neutron energy spectra for intermediate excitation energies is developed. The final state of the residual nucleus may be either discrete or in the continuum. Calculated neutron energy distributions for aluminum are presented.

NASA — GEORGE C. MARSHALL SPACE FLIGHT CENTER

PRECEDING PAGE BLANK NOT FILMED.

TABLE OF CONTENTS

Page

INTRODUCTION 1

Space Vehicle Radiation Shielding 1
Nuclear Reaction Mechanisms for Inelastic Scattering 1

THE COMPOUND NUCLEUS 2

THE HAUSER-FESHBACH MODEL 3

NUCLEAR LEVEL DENSITY 7

Energy Distribution 7
Angular Momentum Distribution 8
Parity Distribution 10

THE OPTICAL MODEL 10

CALCULATIONS 12

REFERENCES 21

LIST OF ILLUSTRATIONS

Figure	Title	Page
1.	Approximately Calculated Continuum Energy Distribution and Eighteen Discrete Transitions for Inelastically Scattered Neutrons with an Incident Energy of 9 MeV	14
2.	Approximately Calculated Continuum Energy Distribution and Ten Discrete Transitions for Inelastically Scattered Neutrons with an Incident Energy of 9 MeV	15
3.	Approximately Calculated Continuum Energy Distribution and Eight Discrete Transitions for Inelastically Scattered Neutrons with an Incident Energy of 12 MeV	16
4.	Exactly Calculated Energy Distribution of Inelastically Scattered Neutrons for an Incident Energy of 15 MeV	17
5.	Exactly Calculated Energy Distribution of Inelastically Scattered Neutrons for an Incident Energy of 18 MeV	18
6.	Exactly Calculated Energy Distribution of Inelastically Scattered Neutrons for an Incident Energy of 21 MeV	19
7.	Comparison of Exactly and Approximately Calculated Energy Distribution for an Incident Energy of 18 MeV	20

LIST OF TABLES

Table	Title	Page
I.	Discrete Transitions of Inelastically Scattered Neutrons for an Incident Energy of 5 MeV	13

DEFINITION OF SYMBOLS

Primes refer to the final state.

c	The set of quantum numbers $\{\alpha, I, i, s, \ell, J, M_J, \pi\}$ which specifies the reaction channel.
α	The set $\{p, E_p\}$ which labels a pair of particles and their state of excitation.
p	The pair of particles.
E_p	The center-of-mass kinetic energy of the pair p.
E_p^*	The energy of excitation of the pair p.
S_p	The separation energy of the pair p from the compound system.
Q	The energy released by the reaction.
I	The intrinsic spin of the target. All spins are in units of $\hbar$, Planck's constant divided by 2π.
i	The intrinsic spin of the bombarding particle.
$\bar{s}$	The channel spin; $\bar{s} = \bar{I} + \bar{i}$.
$\bar{\ell}$	The orbital angular momentum of the pair.
$\bar{J}$	The total angular momentum; $\bar{J} = \bar{\ell} + \bar{s} = \bar{\ell} + \bar{I} + \bar{i}$.
M_J	The z component of J.
π	The total parity (the product of $(1)^{-\ell}$ with the intrinsic parities of the pair α).
$G_{\alpha'}^{J\pi}$	Let the decay and production of compound systems for fixed J and π be equal, so that at any time there are N systems present. Then $NG_{\alpha'}^{J\pi}/\hbar$ is the number of decays per second into the pair α'.

k	The wave number for the relative motion of the pair α.
$\rho_c(E^*, I)$	The number of states in the continuum with angular momentum I and excitation energy in dE^* at E^*.
$\rho_d(E^*, I)$	The level density for discrete states.
$\bar{\sigma}^c_{\alpha\alpha'}$	The average cross section with the residual nucleus excited into the continuum region.
$\bar{\sigma}^d_{\alpha\alpha'}$	The average cross section for a discrete final state.
E_c	If $E_p < E_c$ the residual nucleus will be in a discrete state. If $E_p > E_c$ the residual nucleus will be excited into the continuum region.
$H(X)$	For any X if $X < 0$ then $H(X) = 0$. If $X > 0$ then $H(X) = 1$.
K	The moment of inertia of the nucleus.
C'	A constant depending upon the given nucleus.
G_N	The density of neutron orbits at the Fermi level.
G_z	The density of proton orbits at the Fermi level.
G	The total density of orbits at the Fermi level.
θ	The nuclear "temperature," not to be confused with the "temperature" in the simple evaporation model.
U	The Fermi energy; the excitation energy above the completely degenerate state.
A	The atomic mass number.
J_{iz}	The z - component of angular momentum of the i^{th} particle or hole.

$\langle X \rangle$	The average value of X.
$f(U_\nu)$	The probability density function of U_ν
$g(J_z)$	The probability density function of J_z.
m	The reduced mass of the pair
V	The real part of the optical model potential
W	The imaginary part of the optical model potential
ψ	The total wave function
∇^2	The Laplacian
D(U)	The nuclear energy level density according to the Fermi gas model

INTRODUCTION

Space Vehicle Radiation Shielding

Space vehicles are exposed to proton fluxes produced by solar flares, galactic cosmic sources, and the trapped radiation belts [1]. Proton collisions with the vehicle produce secondary neutrons which are then involved in subsequent nuclear reactions. At neutron energies between 8 and 18 MeV about one half of these secondary neutrons will initiate inelastic neutron scattering reactions. The energy spectra of these inelastically scattered neutrons is required as part of the input for Monte Carlo calculations which predict the radiation dose rate inside the space vehicle.

Nuclear Reaction Mechanisms for Inelastic Scattering

The first problem of nuclear reaction analysis is to establish the mechanism of the interaction. The reaction mechanism is determined by the number of particles which share the energy introduced into the target nucleus. Nuclear reactions are classified for convenience as direct, intermediate, and statistical reactions.

If only a few degrees of freedom of the target nucleus are excited, then the reaction is direct [2]. The momentum transferred to the residual nucleus is small. This commonly results in angular distributions with large asymmetric peaks in either the forward or the back angles.

Doorway or intermediate mechanism states are formed as additional nucleons share the energy [3]. The doorway states may either collapse rapidly to single-particle states or proceed to more complicated configurations. Reactions which go to completion via energy excitations of intermediate complexity have not received adequate theoretical treatment.

If the complexity of the intermediate state continues to increase, then ultimately all nucleons in the nucleus share the available energy. Thus a compound nucleus is formed [4]. The angular distributions resulting from compound nucleus decay are symmetric about 90° in the center-of-mass system.

At present only two of these three types are available for treating inelastic scattering: the direct reaction theory and the compound nucleus or statistical theory. In this report it is assumed that the inelastic neutron scattering proceeds via compound nucleus formation.

THE COMPOUND NUCLEUS

A compound nucleus is a metastable system which is formed when an incident particle is captured by a target nucleus, and the available energy is shared by all nucleons in the system. If one makes the Bohr [5] assumption that the compound nucleus is analogous with an equilibrium system in classical thermodynamics, then the decay of the compound nucleus should be independent of the mode of creation. This assumption leads to a factorization of the reaction cross section into two independent elements (assuming a fixed total angular momentum). The first of these is the cross section for the formation of the metastable compound system, and the second is the probability for subsequent decay through the channel of interest. In this report only the exit channel containing the inelastically scattered neutron is considered.

If no external magnetic fields are present, a time-reversed state must also satisfy the equations of motion which govern the decay of the compound system. This symmetry is expressed mathematically by the reciprocity theorem [4]. The reciprocity theorem in conjunction with the Bohr assumption allows the compound nucleus decay probability to be expressed in terms of the compound nucleus formation cross section for the inverse reaction. In the inverse reaction the target is in an excited state and there is no way to experimentally measure the inverse compound nucleus formation cross section. It is assumed that this cross section is the same as the compound nucleus formation cross section for a target nucleus in the ground state.

These assumptions allow the inelastic neutron cross section to be expressed in terms of the initial state compound nucleus formation cross section. The compound nucleus formation cross section is approximated by the optical model [6] reaction cross section.

For a given excitation energy several states in the compound nucleus will contribute to the total reaction amplitude. The statistical hypothesis [7] assumes that the interference terms between the different transition amplitudes cancel.

The compound nucleus decay probability also contains a term which represents the available final-state phase space. It is normally assumed that the density of final states of the residual nucleus depends upon the excitation energy and spin, but is independent of the parity of the state. The energy and spin dependence are usually separated into independent multiplicative factors.

The energy dependence is approximated by using the Fermi gas model of the nucleus [8], and the spin dependence for multiparticle excited states is approximated by a Gaussian distribution [9].

Thus the inelastic neutron cross section is expressed in terms of functions which are determined by optical model and level density parameters. The physical implications and validity of the above assumptions will be discussed in the sections which follow.

THE HAUSER-FESHBACH MODEL

Early evaporation models which were developed by Bethe and Weisskopf considered only conservation of energy. The Hauser-Feshbach [10] model presented below includes conservation of total angular momentum and parity.

The incident neutron energies are spread over some small energy interval. This implies excitation of compound states within a corresponding energy interval. The statistical assumption states that there are many excited states in this interval, and the widths and energies of the excited states are randomly distributed within this energy interval. The cross section calculated is the average over individual resonances in this energy interval.

Let $\bar{\sigma}_{\alpha\alpha'}$ be the average angle-integrated cross section for transition from state α to state α'. This cross section is the sum over all partial cross sections, $\sigma^{J\pi}_{\alpha\alpha'}$, which conserve angular momentum, J, and parity, π.

$$\bar{\sigma}_{\alpha\alpha'} \equiv \sum_{J\pi} \sigma^{J\pi}_{\alpha\alpha'} \tag{1}$$

It is assumed that each partial cross section may be factored into two factors. The first factor is the cross section for the formation of the compound nucleus, $\sigma^{J\pi}_{c}(\alpha)$, and depends only upon the initial state. The second factor is the branching ratio, $G^{J\pi}_{\alpha'} / \sum_{\alpha''} G^{J\pi}_{\alpha''}$, and depends only upon the final state.

$$\bar{\sigma}^{J\pi}_{\alpha\,\alpha'} = \sigma^{J\pi}_{c}(\alpha)\, G^{J\pi} / \sum_{\alpha''} G^{J\pi}_{\alpha''} \tag{2}$$

The reciprocity theorem may be used to express the branching ratio in terms of the compound-nucleus-formation cross section.

$$k^2_{\alpha}\, \bar{\sigma}^{J\pi}_{\alpha\,\alpha'} = k^2_{\alpha'}\, \bar{\sigma}^{J\pi}_{\alpha'\alpha} \tag{3}$$

From equations (2) and (3) one obtains

$$k^2_{\alpha}\, \sigma^{J\pi}_{c}(\alpha)\, G^{J\pi}_{\alpha'} / \sum_{\alpha''} G^{J\pi}_{\alpha''} = k^2_{\alpha'}\, \sigma^{J\pi}_{c}(\alpha)\, G^{J\pi}_{\alpha} / \sum_{\alpha''} G^{J\pi}_{\alpha''} \quad .$$

Equating terms in α gives

$$G^{J\pi}_{\alpha} = k^2_{\alpha}\, \sigma^{J\pi}_{c}(\alpha) \tag{4}$$

Each $\sigma_c(\alpha)$ is obtained from the optical-model absorption cross section, $\sigma_{\alpha a}$.

$$\sigma_{\alpha a} \equiv \sum_{J\pi} \sigma^{J\pi}_{c}(\alpha) \tag{5}$$

In terms of the optical-model complex phase shifts, $\delta_{\alpha\ell}$ this is

$$\sigma_{\alpha a} = (\pi / k^2_{\alpha}) \sum_{\ell} (2\ell + 1)(1 - |\exp 2i\,\delta_{\alpha\ell}|^2) \quad , \tag{6}$$

where ℓ is the orbital angular momentum of the interacting particles. For the partial cross sections one has

$$\sigma^{J\pi}_{c}(\alpha)$$

$$= [\pi\,(2J + 1)/k^2_{\alpha}\,(2I + 1)(2i + 1)] \sum_{S=|I-i|}^{I+i} \sum_{\ell=|J-S|}^{J+S} (1 - |\exp 2i\,\delta_{\alpha\ell}|^2) \quad . \tag{7}$$

The transmission functions are defined by

$$T_\ell(\alpha) \equiv 1 - |\exp 2i\,\delta_{\alpha\ell}|^2 . \tag{8}$$

Thus, from equations (4), (7), and (8), one finds

$$G_\alpha^{J\pi} = [\pi(2J+1)/(2I+1)(2i+1)] \sum_{\ell,s} T_\ell(\alpha) . \tag{9}$$

From equation (2),

$$\bar{\sigma}_{\alpha\alpha'}^{J\pi} = [\pi(2J+1)/k_\alpha^2(2I+1)(2i+1)] \sum_{\ell,s} T_\ell(\alpha) \left[G_{\alpha'}^{J\pi} \Big/ \sum_{\alpha''} G_{\alpha''}^{J\pi} \right] . \tag{10}$$

From equations (1), (9), and (10),

$$\bar{\sigma}_{\alpha\alpha'}$$

$$= (\pi/k_\alpha^2) \sum_{J,\pi} [(2J+1)/(2I+1)(2i+1)] \sum_{s,\ell} T_\ell(\alpha) \left[\sum_{s,\ell'} T_{\ell'}(\alpha) \Big/ \sum_{\alpha'' s'' \ell''} (\alpha'') \right] . \tag{11}$$

Since it is not possible to define the final energy more accurately than the initial energy, there is an energy interval associated with the final state. If the compound system is highly excited, then the residual nucleus is likely to be highly excited also. For a highly excited residual nucleus the level density is represented by a continuous density function. However, if the compound nucleus has a lower excitation energy, then the residual nucleus may be in a discrete energy state. In general there will be some transitions to continuous final states and some transitions to discrete final states. The experimentally measured neutron spectrum is the average cross section times the number of final states in the energy interval. Thus the energy spectrum of neutrons emitted from the compound nucleus is

$$N(E_{p'}) = \rho_c(E^*, I')\,\bar{\sigma}_{\alpha\alpha'}^{c} H(E_c - E_{p'}) + \rho_d(E^*, I')\,\bar{\sigma}_{\alpha\alpha'}^{d} H(E_{p'} - E_c) , \tag{12}$$

where H is the Heaviside function.

The discrete density of states, ρ_d, is unity if $dE_{p'}$ is chosen so small that only one final discrete state is excited. The continuous density of states, ρ_c, is taken to be the form

$$\rho_c(E^*, I) = \rho(E^*)(2I + 1) \exp[-I(I + 1)/2\sigma^2] \tag{13}$$

The above spin level-density formula predicts too many levels of high spin at low energies. All levels of high spin at low energies should be excluded if they are not energetically obtainable by adding rotation energy to the ground state. If this spin cutoff is included the neutron energy spectrum becomes

$$N(E_{p'})$$

$$= \left[(\pi/k_\alpha^2) \sum_{J\pi} g_J \left[\sum_{s\ell} T_\ell(\alpha) \right] \sum_{\ell'} g_{\ell' Jp'} T_{\ell'}(E_{p'}) \, [H(E_c - E_{p'}) \rho_c(E_{p'}^{max} - E_{p'})] \right.$$

$$\left. + (\pi/k_\alpha^2) \sum_{J\pi} g_J \left[\sum_{s\ell} T_\ell(\alpha) \right] \sum_{s'\ell'} T_{\ell'}(E_{p'}) \, H(E_{p'} - E_c) \right] \tag{14}$$

$$\div \left[\sum_{p''\ell''} \int_0^{E_c} g_{\ell'' Jp''} T_\ell(E_{p''}) \, \rho_c \, (E_{p''}^{max} - E_{p''}) \, dE_{p''} \right.$$

$$\left. + \sum_{\alpha'' s'' \ell''} T_{\ell''}(E_{p''}) \, J(E_{p''} - E_c) \right]$$

where $\quad g_J \equiv (2J + 1)/(2I + 1)(2i + 1)$

$$g_{\ell' Jp'} \equiv \sum_{\pi' s' I'} 2(I + 1) \exp[-I'(I' + 1)/2K] \, H[(E_{p'}^{max} - E_{p'})$$

$$- \hbar^2 I'(I' + 1)/2K] \; .$$

NUCLEAR LEVEL DENSITY

The inelastic neutron energy spectrum contains a factor which represents the available final-state phase space. For a two-body reaction, the phase space factor is determined predominately by the level density in the residual nucleus.

Nuclear level densities exhibit an essentially exponential increase with excitation energy. This rapid increase may be basically explained as a result of the addition of many elementary one-particle excitations to form a highly excited many-particle level. This is a characteristic of the Fermi gas model which only required that the excitation energy of the level be distributed among several excited nucleons in a manner consistant with the Pauli principle.

Nuclear level densities are strongly influenced by nuclear shell structure. In particular, for a fixed excitation energy, the level densities of magic nuclei are orders of magnitude smaller than the level densities of adjacent nuclei.

Odd-even effects which are attributed to differences in pairing energies are also present. At low excitation energies, the odd nuclei often exhibit several shell model levels, but even nuclei have few levels in this region of excitation. Above the region of collective excitations, the even nuclei have many levels which arise from the numerous ways in which unpaired nucleons can be arranged.

The above effects are most pronounced at low energies and decrease with increasing excitation. However, these factors do not entirely disappear and must be considered in any satisfactory theory of nuclear level densities.

Energy Distribution

Models which describe nuclear level densities must be related to both the Fermi gas model and to the shell model. The odd-even effect indicates an additional complexity. Newton [8] has considered the nucleus as a Fermi gas and included shell effects by replacing the density of nucleon orbits at the Fermi level by the density of nucleon orbits in the shell model. The equivalent energy of the Fermi gas is obtained by subtracting the pairing energy correction from the nuclear excitation energy. In this model the level density is

$$D(U) = C' A G_Z^{1/2} G_N^{1/2} (2U + 3\theta)^2 \exp[-2(\pi^2 G U/6)^{1/2}] \,,$$

where $\theta = \left(\frac{6U}{\pi^2 G}\right)^{1/2}$ and $G = G_N + G_Z$. (15)

Effective values of G for various nuclei have been tabulated by Cameron [11].

Angular Momentum Distribution

Consider a Fermi gas with ν excited holes and particles. The projection of the total angular momentum on the Z-axis of the system is

$$J_z = \sum_{i=1}^{\nu} J_{iz} \,. \tag{16}$$

The random variables $J_{1z}, \ldots, J_{\nu z}$ are independent and have the same distribution with standard deviation $\sigma_\nu \neq 0$.

$$\langle J_{iz} \rangle = 0$$

$$\langle J_{iz}^2 \rangle = \sigma_\nu^2 \tag{17}$$

Define the arithmetic mean of the ν independent random variables as

$$U_\nu = J_z/\nu \,. \tag{18}$$

It immediately follows from the central limit theorem [12] that U_ν has an asymptotically normal distribution with mean $\langle J_{iz} \rangle$ and standard deviation $\sigma_\nu/\sqrt{\nu}$.

The normal distribution is defined by

$$f(x) = \frac{1}{\sqrt{2\pi \langle x^2 \rangle}} \exp\left[- \frac{(x - \langle x \rangle)^2}{2 \langle x^2 \rangle}\right] \tag{19}$$

and

$$f(U_\nu) = \frac{1}{\sqrt{2\pi\ \sigma_\nu^2/\nu}} \exp\left[-\frac{U_\nu^2}{2\sigma_\nu^2/\nu}\right] . \tag{20}$$

Since $f(U_\nu)\, dU_\nu = g(J_z)\, dJ_z$ it follows that

$$g(J_z) = \frac{f(U_\nu)}{\nu} = \frac{1}{\sqrt{2\pi\,\nu\sigma_\nu^2}} \exp\left[\frac{-J_z^2}{2\nu\sigma_\nu^2}\right] . \tag{21}$$

The density of states of spin I, $\rho(I)$, is the difference between the level density of spin $J_z = I$ and $J_z = I + 1$.

$$\rho(I) = g(I) - g(I+1) \simeq \frac{(2I+1)}{2(2\pi)^{1/2}\sigma^3} \exp[-I(I+1)/2\sigma^2] \tag{22}$$

The parameter $\sigma^2 = \nu\sigma_\nu^2$ is called a spin cutoff parameter, which must be determined for a given nucleus. The spin cutoff is a function of the Fermi energy. However, σ is normally taken to be constant, since if it is energy dependent, the energy integrals and spin sums in the neutron inelastic energy spectrum cannot be separated.

If $\rho(I)$ is energy independent, then it predicts the same ratio of high-spin states and low-spin states at all excitation energies. This is incorrect since high spin states do not appear at low energies. The low-lying levels are shell model states of low angular momentum. Rotational bands are built upon these low-lying states, and the rotational energy determines the high-spin states. The rotational energy is given by

$$E_r = (\hbar^2/2K)\, I(I+1) . \tag{23}$$

If this rotational energy is added to the ground state, then E_r determines the energy level at which a high-spin state first appears. This fact is represented in the neutron inelastic energy spectrum by an energy cutoff which prohibits high spins at low energies.

Parity Distribution

Single Fermion states have parity (+1) or (-1). The resulting parity of the system may be determined from elementary probability considerations. It may be shown that only a small number of negative parity states or a small number of positive parity states are required to obtain a nearly equal probability for positive and negative total parity.

THE OPTICAL MODEL

The optical model represents the interaction of a nucleon with the nucleus in terms of a single-particle complex potential. The real part of the potential describes the scattering of nucleons; the imaginary part describes absorption.

The Schroedinger equation for neutrons can be written as

$$\nabla^2 \psi + \frac{2m}{\hbar^2} [E - (V + iW)] \psi = 0 .$$

The solution is obtained by expanding ψ in terms of Legendre polynomials.

$$\psi = \sum_{\ell} \psi_\ell (r) \; P_\ell (\cos\theta) .$$

Then $\psi_\ell(r)$ satisfies the equation

$$\frac{1}{r^2} \frac{d}{dr} \left(r^2 \frac{d\psi_\ell}{dr} \right) + \frac{2m}{\hbar^2} [E - (V + iW)] \psi_\ell - \frac{\ell(\ell+1)}{r^2} \psi_\ell = 0 .$$

The general solution of this equation which asymptotically approaches the equation of a free particle is of the form

$$\psi_\ell = C_\ell \psi_\ell^{I} + C_2 \psi_\ell^{II} .$$

The boundary condition at the origin is

$$\lim_{r \to 0} [r \psi_\ell (r)] = 0 .$$

This condition determines the complex phase shifts $\delta_{\alpha \ell}$ which are defined by

$$\frac{C_1}{C_2} = \exp(2i\,\delta_{\alpha\ell}) \equiv \eta_\ell = \lim_{r \to 0} \frac{-r\,\psi_\ell^{II}}{r\,\psi_\ell^{I}} \quad .$$

The asymptotic expansion is

$$\psi_\ell = C_2 \left\{ \left(\psi_\ell^{II} + \psi_\ell^{I} \right) - [1 - \exp(2i\,\delta_{\alpha\ell})]\,\psi_\ell^{I} \right\} \quad .$$

The first term represents the ℓ^{th} term in the incident plane wave expansion. The second term is the ℓ^{th}-order scattered wave.

The reaction cross section, σ_r, is the ratio N_a/N, where N_a is the net flux into a large sphere of radius r_0 as computed from the complete wave function, and N is the incident plane wave flux.

$$\sigma_r = \frac{\hbar^2}{2imV} \int \left(\frac{\partial \psi}{\partial r}\psi^* - \frac{\partial \psi^*}{\partial r}\psi \right) r_0^2 \sin\theta \, d\theta \, d\phi \quad .$$

The cross section calculated by the optical model is an average cross section over an energy region containing many resonance levels. The optical model is satisfactory when the width of the beam is considerably larger than the level spacing. Thus, over an energy interval containing many resonances,

$$\bar{\eta}_\ell = \frac{\int_{\Delta E} \eta_E \, dE}{\Delta E} \quad .$$

The average reaction cross section is

$$\bar{\sigma}_r = \frac{\pi}{k_\alpha^2} \sum_\ell (2\ell + 1)(1 - \overline{|\eta_\ell|^2})$$

or

$$\sigma_r = \frac{\pi}{k_\alpha^2} \sum_\ell (2\ell + 1) \left[(1 - |\bar{\eta}_\ell|^2) - (\overline{|\bar{\eta}_\ell - \eta_\ell|^2}) \right] \quad .$$

The second term results from resonance reactions for which η_ℓ differs significantly from $\bar{\eta}_\ell$. The first term is the absorption cross section for compound nucleus formation, i.e., the absorption results in formation of a compound system with excitation energy in a region which contains many resonance levels. Thus

$$\sigma_{\alpha a} = \frac{\pi}{k_\alpha^2} \sum_\ell (2\ell + 1)(1 - |\bar{\eta}_\ell|^2) \quad .$$

Various functional forms have been used to approximate the optical model potential 6, 11. For incident energies between 5 and 10 MeV, it is best to work with diffuse boundary potentials. In this case, it is necessary to use a computer in order to solve the Schroedinger equation and obtain the phase shifts.

CALCULATIONS

The inelastic neutron cross section for aluminum for an incident energy of 5 MeV is composed primarily of transitions to discrete energy levels. The results of the computer program ABACUS [12] for an incident energy of 5 MeV are presented in Table I.

As the incident energy increases the transitions are to both discrete final states and final states in the continuum. Figures 1 and 2 show these mixed transitions at 9 MeV for 18 and 10 discrete levels, respectively. Figure 3 is the result for an incident energy of 12 MeV.

At higher incident energies the cross section is dominated by transitions to the continuum. Figures 4, 5, and 6 include continuum transitions only.

Figures 1 through 6 are not the neutron energy spectra as represented by Equation (14), but are a composite of ABACUS and a computer code developed by R. Snow and M. C. George [13]. The curves are all normalized to an integrated cross section of 0.8 barns. Some of the options available in the continuum code are indicated in Figure 7.

TABLE I. DISCRETE TRANSITIONS OF INELASTICALLY SCATTERED NEUTRONS FOR AN INCIDENT ENERGY OF 5 MeV

DISCRETE ENERGY LEVELS (MeV)	CROSS SECTION (BARNS)
0.842	0.053547
1.013	0.109156
2.212	0.173929
2.731	0.116153
2.976	0.064010
3.010	0.187355
3.674	0.022831
3.951	0.045302
4.052	0.017250

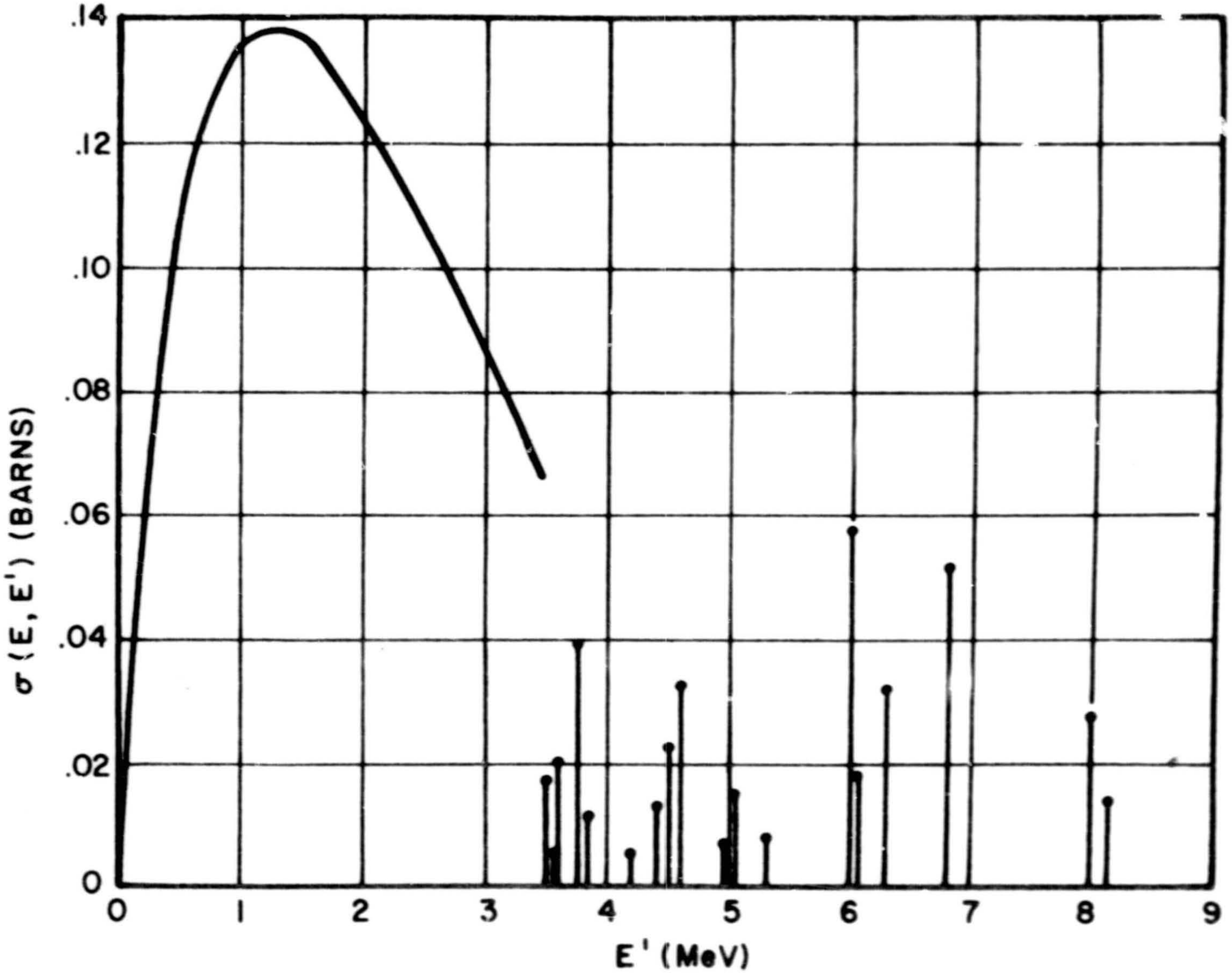

FIGURE 1. APPROXIMATELY CALCULATED CONTINUUM ENERGY DISTRIBUTION AND EIGHTEEN DISCRETE TRANSITIONS FOR INELASTICALLY SCATTERED NEUTRONS WITH AN INCIDENT ENERGY OF 9 MeV

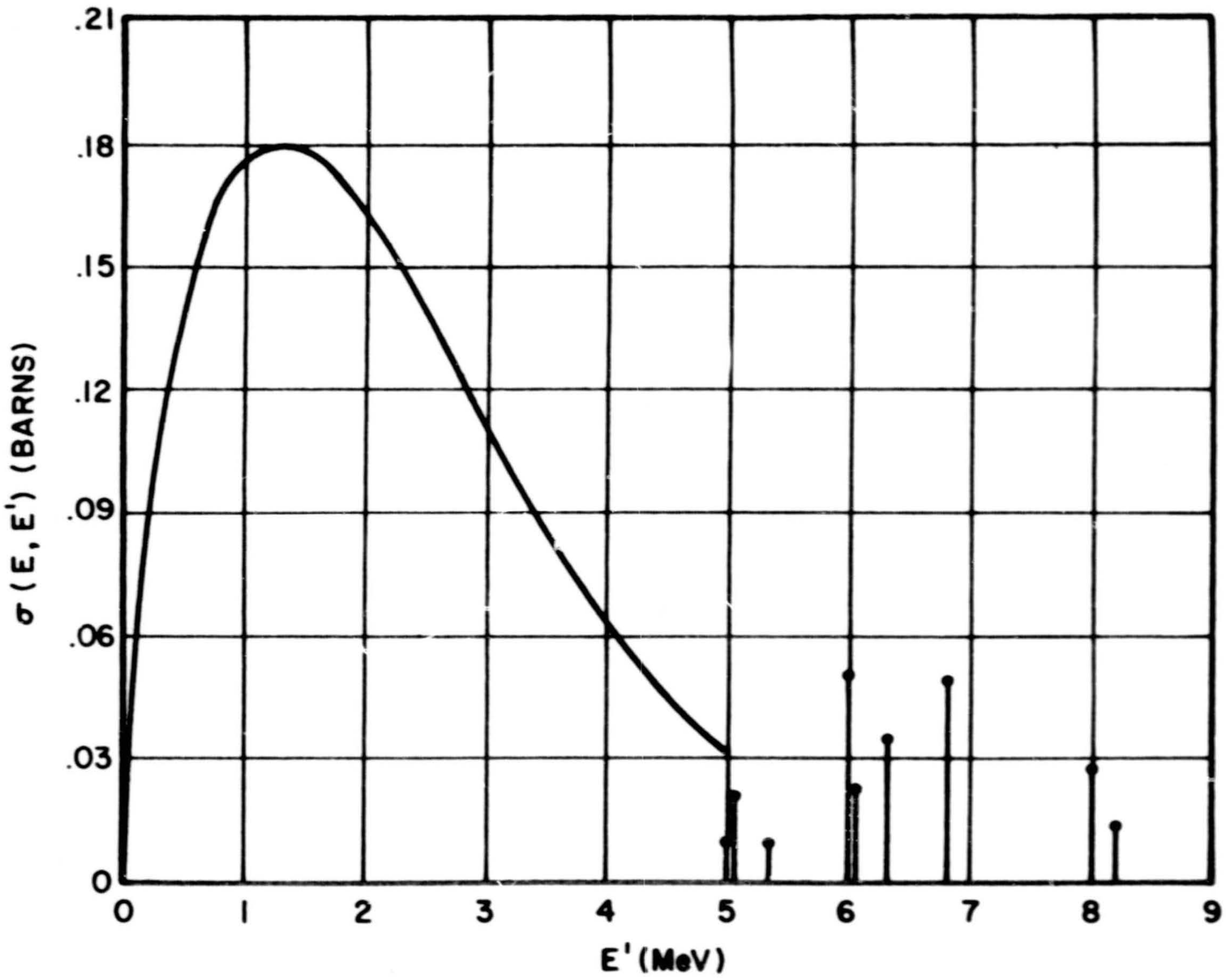

FIGURE 2. APPROXIMATELY CALCULATED CONTINUUM ENERGY DISTRIBUTION AND TEN DISCRETE TRANSITIONS FOR INELASTICALLY SCATTERED NEUTRONS WITH AN INCIDENT ENERGY OF 9 MeV

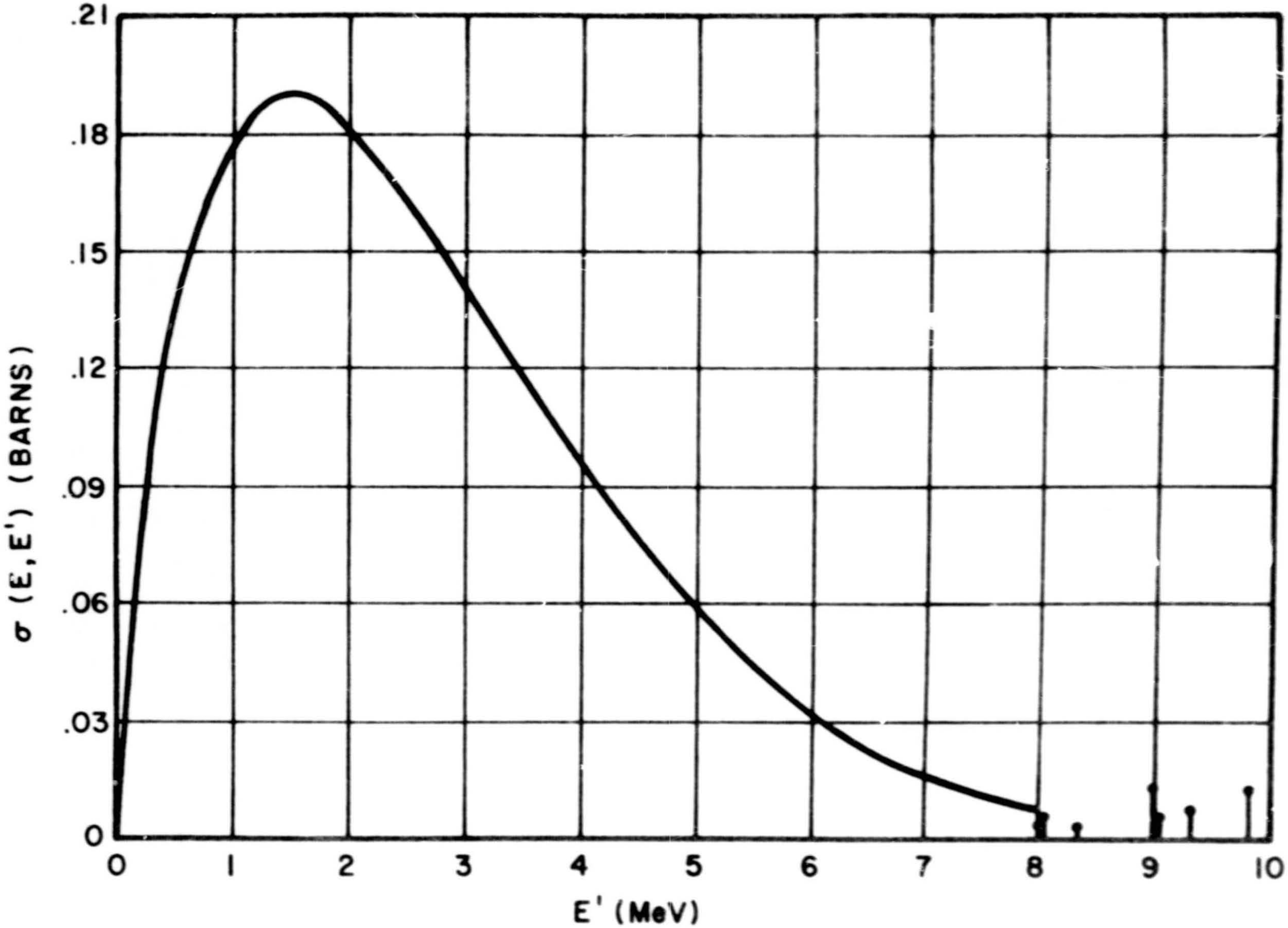

FIGURE 3. APPROXIMATELY CALCULATED CONTINUUM ENERGY DISTRIBUTION AND EIGHT DISCRETE TRANSITIONS FOR INELASTICALLY SCATTERED NEUTRONS WITH AN INCIDENT ENERGY OF 12 MeV

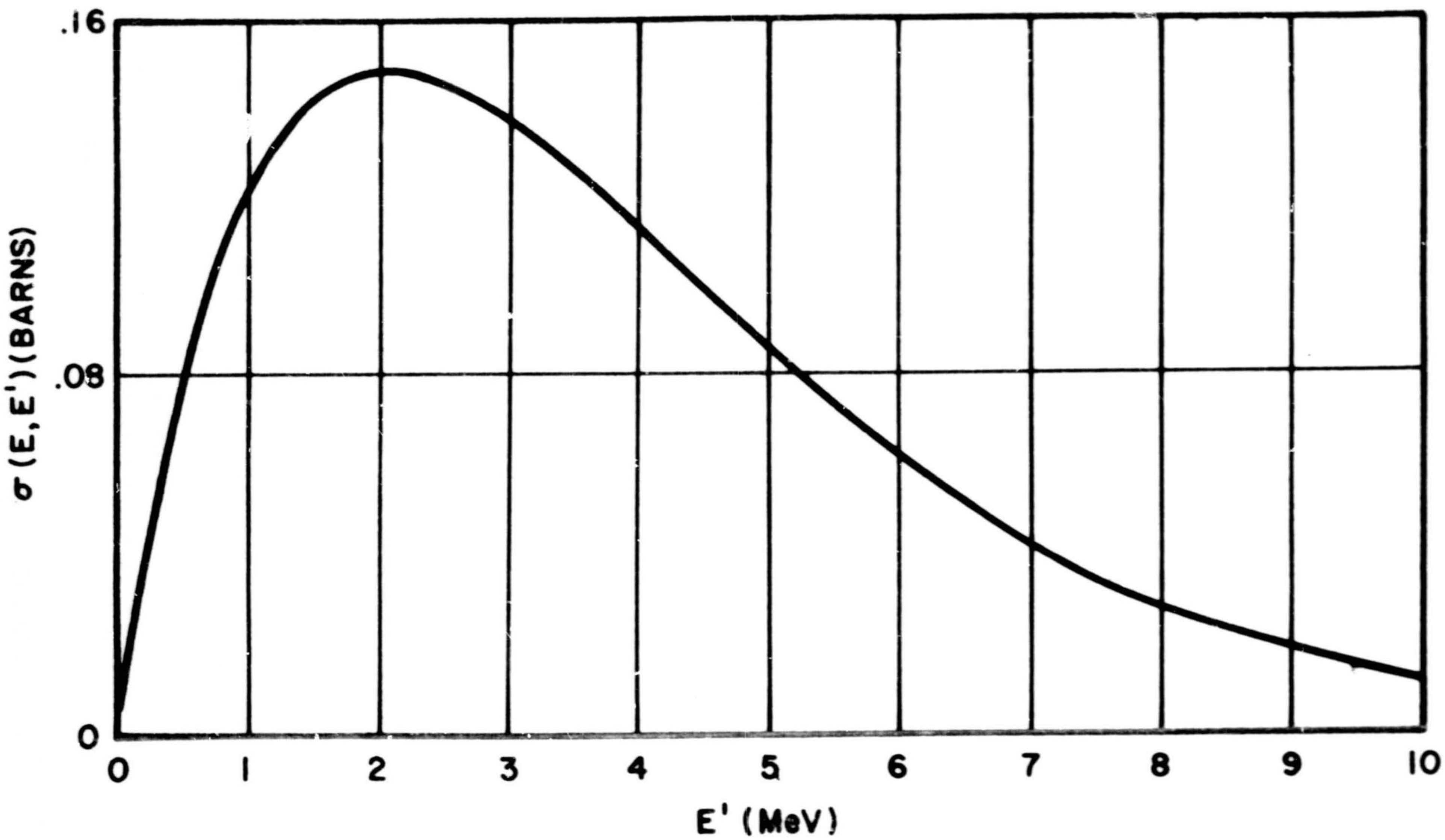

FIGURE 4. EXACTLY CALCULATED ENERGY DISTRIBUTION OF INELASTICALLY SCATTERED NEUTRONS FOR AN INCIDENT ENERGY OF 15 MeV

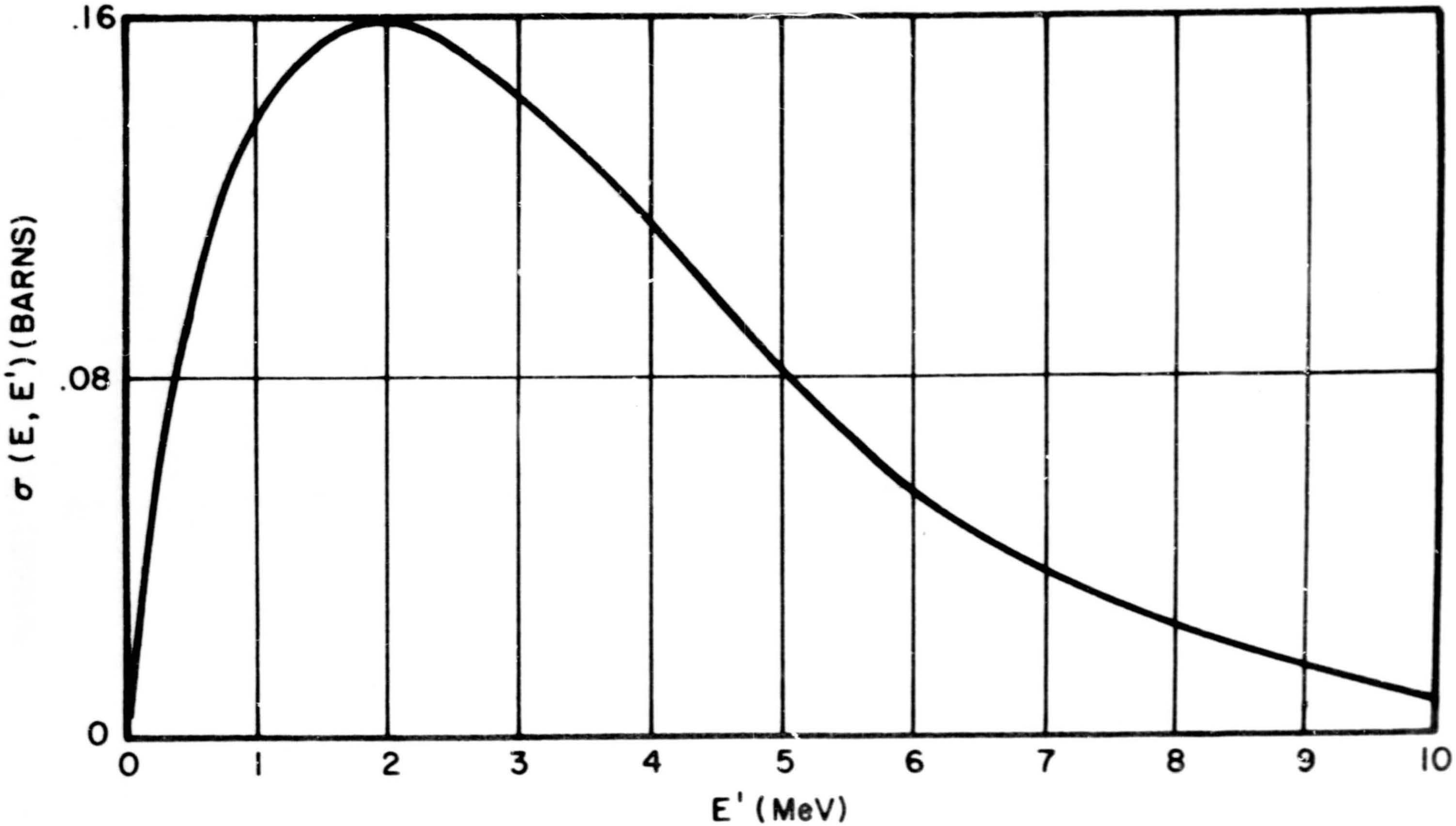

FIGURE 5. EXACTLY CALCULATED ENERGY DISTRIBUTION OF INELASTICALLY SCATTERED NEUTRONS FOR AN INCIDENT ENERGY OF 18 MeV

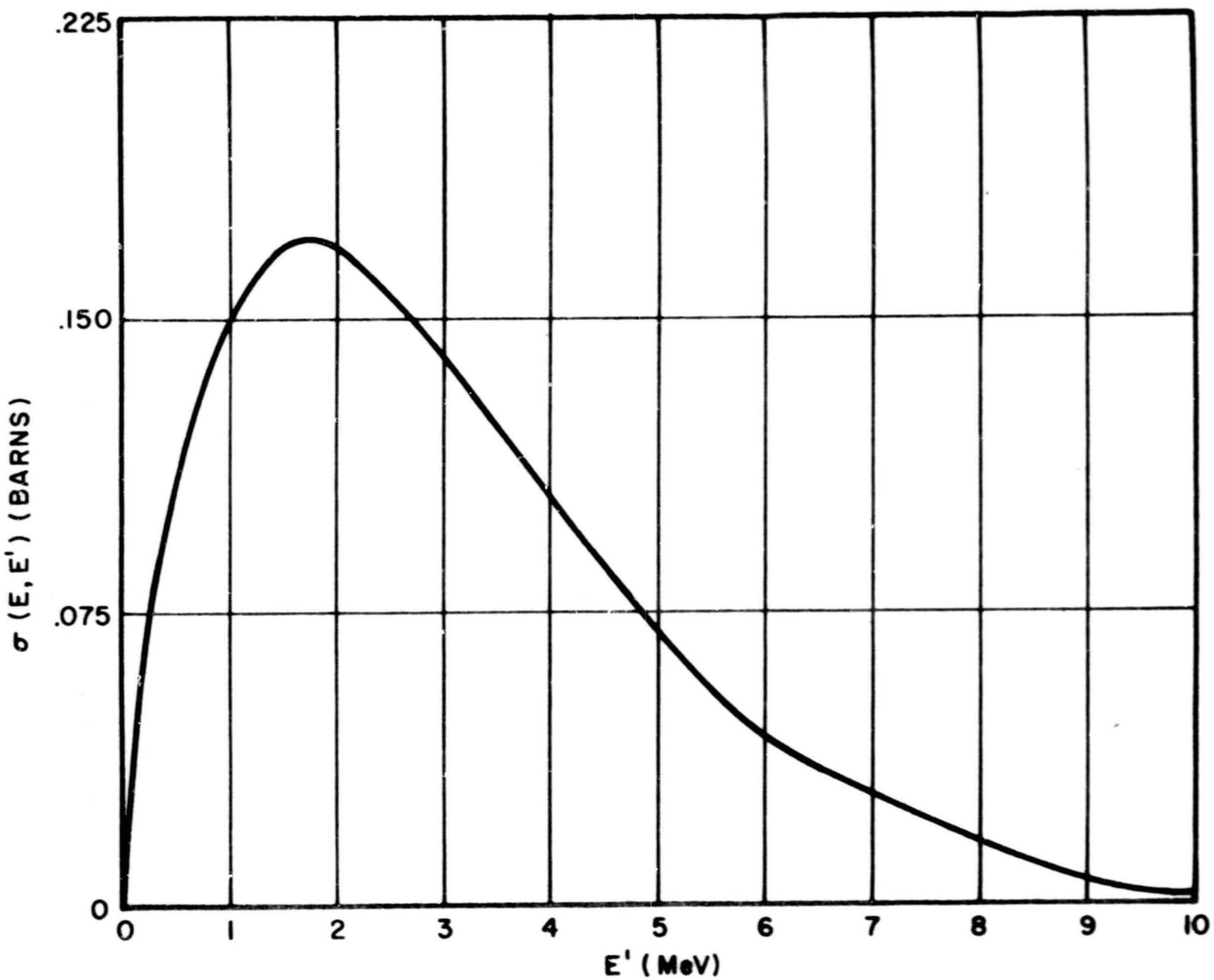

FIGURE 6. EXACTLY CALCULATED ENERGY DISTRIBUTION OF INELASTICALLY SCATTERED NEUTRONS FOR AN INCIDENT ENERGY OF 21 MeV

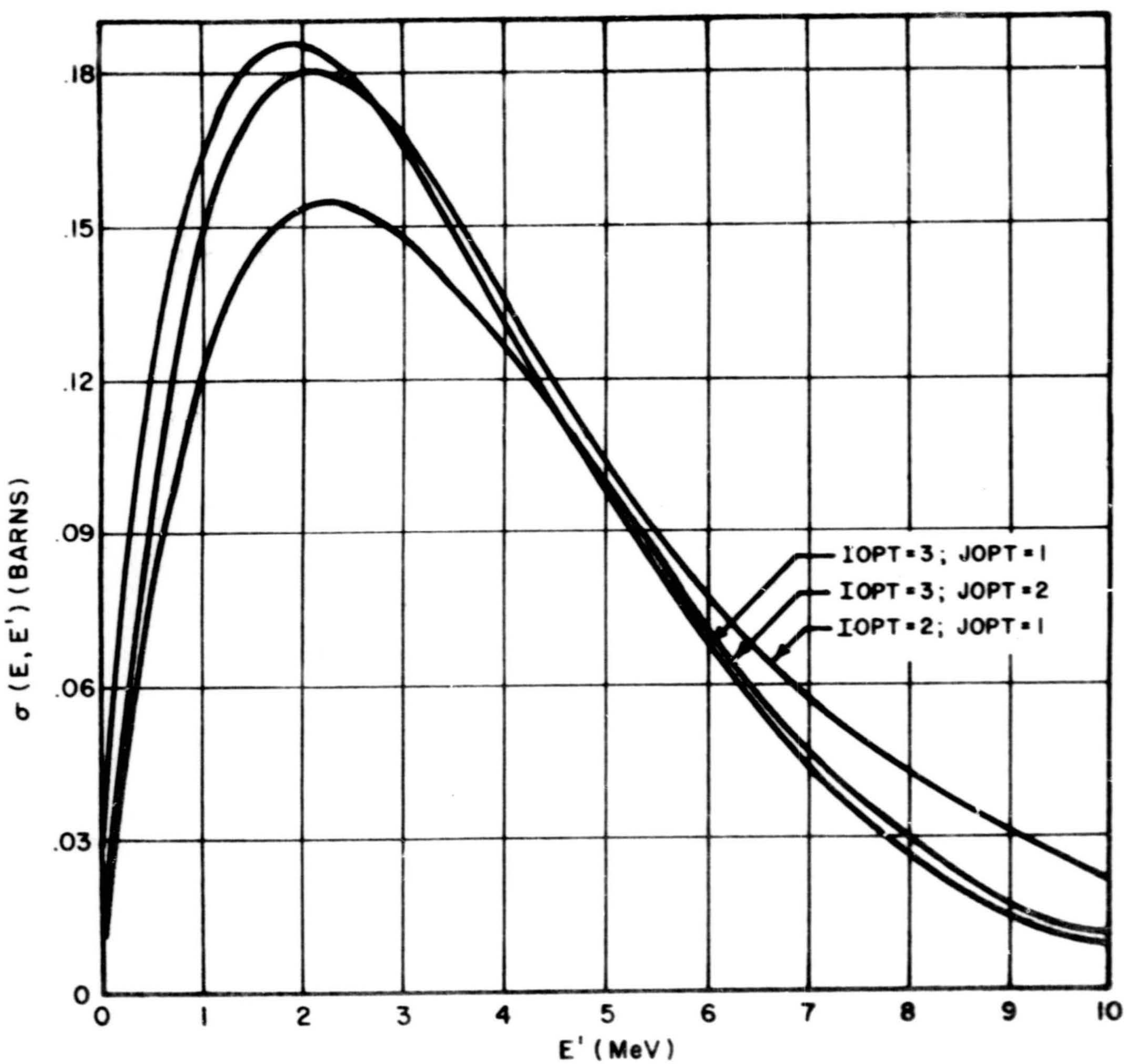

FIGURE 7. COMPARISON OF EXACTLY AND APPROXIMATELY CALCULATED ENERGY DISTRIBUTION FOR AN INCIDENT ENERGY OF 18 MeV

REFERENCES

1. Burrell, M. O., Wright, J. J., and Watts, J. W.: An Analysis of Energetic Space Radiation and Dose Rates. NASA TN D-4404, 1968.

2. Tobocman, W.: Theory of Direct Nuclear Reactions. Oxford University Press, New York, 1961.

3. Feshbach, H.: Ann. Phys. (N. Y.) Vol 5, 1958, p. 357.

4. Blatt, J., and Weisskopf, V. F.: Theoretical Nuclear Physics. John Wiley and Sons, Inc., New York, 1952.

5. Bohr, N.: Nature. Vol. 137, 1936, p. 344.

6. Úlehla, I., Gomolcák, L., and Pluhar, Z.: Optical Model of the Atomic Nucleus. Academic Press, New York, 1964.

7. Bethe, H. A.: Rev. Mod. Phys., Vol. 9, 1937, p. 69.

8. Newton, T. D.: Can. J. Phys., Vol. 34, 1956, p. 804.

9. Ericson, T.: Advances in Physics, Vol. 9, 1960, p. 425.

10. Hauser, W., and Feshbach H.: Phys. Rev., Vol. 87, 1952, p. 366.

11. Nemirovskii, P. E.: Contemporary Models of the Atomic Nucleus. The Macmillan Company, New York, 1963.

12. Auerbach, E. H.: Report No. BNL 6562, Brookhaven National Laboratory, 1962.

13. Snow, R., and George, M. C., Interim Report RL-SSL-200, Brown Engineering Co., Inc., Huntsville, Alabama, 1968.